

Micro-structured light emission from planar InGaN light-emitting diodes

Author

Massoubre, David, Xie, Enyuan, Guilhabert, Benoit, Herrnsdorf, Johannes, Gu, Erdan, M. Watson, Ian, D. Dawson, Martin

Published

2014

Journal Title

Semiconductor Science and Technology

DOI

[10.1088/0268-1242/29/1/015005](https://doi.org/10.1088/0268-1242/29/1/015005)

Rights statement

© 2014 Institute of Physics Publishing. This is the author-manuscript version of this paper. Reproduced in accordance with the copyright policy of the publisher. Please refer to the journal's website for access to the definitive, published version.

Downloaded from

<http://hdl.handle.net/10072/63926>

Griffith Research Online

<https://research-repository.griffith.edu.au>

Micro-structured light emission from planar InGaN light-emitting diodes

David Massoubre^{1,2}, Enyuan Xie², Benoit Guilhabert²,
Johannes Herrnsdorf, Erdan Gu, Ian M Watson and Martin D Dawson

Institute of Photonics, University of Strathclyde, SUPA, 106 Rottenrow, Glasgow G4 0NW, UK

E-mail: d.massoubre@griffith.edu.au

Received 26 September 2013, in final form 18 October 2013

Published DD MM 2013

Online at stacks.iop.org/SST/28/000000

Abstract

Investigation of the surface modification of the p-type layer in GaN light-emitting diodes (LEDs) by exposure to a trifluoromethane plasma is reported. It is found that the plasma treatment reduces the conductivity of the p-GaN by several orders of magnitude, and when applied at room-temperature through a patterned mask, localized current channels into the active region of a p-i-n device are created. This provides a novel approach to laterally modulate the light emission from an LED over essentially planar areas. This technique allows the projection of high-resolution images from non-pixelated devices, and an example application of maskless pattern transfer with sub-micron features into photoresist is demonstrated.

Q1 (Some figures may appear in colour only in the online journal)

1. Introduction

During the past decade, much work has been devoted to the development of high power gallium nitride (GaN)-based light emitting diodes (LEDs) emitting in the ultraviolet (UV) and visible spectrum. Most of these efforts have concentrated on the improvement of material quality, internal quantum efficiency, and light extraction for general lighting applications [1]. The standard GaN LED fabrication approach is dictated by the use of an insulating substrate material, sapphire. Light-emitting areas are defined as mesas by dry etching of p-i-n epistructures down to the n-layer, resulting in devices with both n- and p-contacts on the same side of the substrate. While mesas can be as large as a few square millimeters for lighting devices, this same basic approach has been extended to fabricate arrays of micro-pixelated LEDs in which individual pixels may be only a few tens of square micrometers in area. Such micro-pixelated LED arrays are currently the main approach to extend the functionality of GaN-based LEDs to advanced applications including image display [2], visible light communications [3], optical tweezers [4], and maskless

lithography [5]. However, the mesa-etching method of defining pixels has its disadvantages. The introduction of defects during dry etching becomes more problematic as the ratio of sidewall area to pixel area increases [6]. Importantly, the resolution of displayed patterns is limited by the pitch of the pixel array. Furthermore, the non-planar surface left by mesa etching may complicate integration of additional elements in lab-on-chip and related microsystems.

Previous work on ion implantation and plasma treatment of GaN-based structures suggests possible approaches for mesa-free definition of emissive areas in GaN LEDs. High-energy ion implantation can increase resistivity in both n- and p-type nitrides, through introduction of trap states [7]. However, implant isolation has not achieved the same uptake for III-nitride as in other III-V materials, and the damage introduced is an obvious drawback for light-emitting devices. The de-activation of p-type Mg-doped GaN through the specific mechanism of Mg-H complex formation is also well known, and can be achieved through proton implantation [8], simple H₂ gas exposure, or plasma treatment [9]. The latter two techniques, however, require additional heating (to at least 300 °C) to allow hydrogen to diffuse to a useful depth from the surface, and therefore cannot be used with photoresist (PR) masks for pattern definition. Kuo *et al* recently reported a method for increasing the contact barrier height to

¹ Present address: Griffith University, Queensland Micro and Nanotechnology Centre, West Creek Road, Nathan Qld 4111, Australia.

² These authors have contributed equally to this work.

p-GaN by exposure to $\text{Cl}_2/\text{BCl}_3/\text{Ar}$ plasmas, compatible with pattern transfer across a broad-area LED mesa [10]. Finally, CF_4 -based plasmas have been applied quite extensively to improve the performance of GaN-based high electron mobility transistors (HEMTs) following the initial work of Cai *et al* [11]. Various effects are believed to contribute, including the implantation of fluorine to depths of ~ 20 nm where it can affect the AlGaIn-GaN heterojunction present in the HEMT structures.

Here we report a novel technique for defining localized current channels in the p-type layer of p-i-n GaN-based LED structures. This process involves application of a CHF_3 -based plasma at room temperature, and has two key characteristics allowing light emission across a macroscopic mesa to be spatially modulated in an arbitrary fashion. Firstly, the effect of the plasma treatment is blocked by conventional PR layers, allowing any micron-scale pattern created in the resist to generate an equivalent pattern of current injection into the LED active region. Secondly, the plasma treatment penetrates through a conventional semi-transparent metal layer, which can be applied over the full mesa surface to spread current from a remote p-contact pad. We discuss the scope of this technique for pattern and image display, illustrating the achievable resolution. We also discuss mechanistic aspects of the process, and demonstrate high-fidelity transfer of patterns in maskless lithography.

2. Experiment

To demonstrate our novel process, broad emitting-area GaN-based LEDs, with peak emission wavelengths at 405 nm and 450 nm respectively, were fabricated following a standard process and using a commercially available p-i-n LED structure grown on a c-plane sapphire wafer. First, the wafer was diced into pieces of appropriate size and cleaned. The samples were next soaked for 3 min in an 18% aqueous HCl solution to remove the native oxide, then rinsed in de-ionized water. This was immediately followed by the deposition with an electron beam evaporator of a bilayer of Ni/Au (15 nm/25 nm) to be used as a current spreading layer. Next, a thin PR layer was spin-coated on each sample and patterned by standard photolithography to define the mesa for each broad emitting-area LED, created by a chlorine-based inductively coupled plasma dry etching step down to the n-doped GaN layer. For a first demonstration, large broad-area mesas with a size of $250 \times 250 \mu\text{m}^2$ were defined. The PR pattern remaining after mesa etching was washed off, and the samples underwent rapid thermal annealing at 500°C for 120 s in a purified air ambient to form semi-transparent ohmic contacts to the p-GaN. This oxidative anneal converts the Ni metal into a conductive NiO_x phase, that is immiscible with the Au component, resulting in a two-phase nanocomposite [12]. Finally, n-pads and p-pads consisting of a 50 nm/200 nm Ti/Au bilayer were deposited by sputtering and patterned by lift-off processing. In order to create the micro-images, an additional step was added to the standard LED process. This additional step, which can be done at any stage after the p-contact annealing, consists of spin-coating a 500 nm-thick

PR (Microposit S1805, positive tone) layer followed by standard photolithography to transfer a micro-pattern from a photo-mask into the PR as schematized in figure 1(a). Subsequently, the patterned samples underwent a room temperature plasma treatment in a reactive ion etch system (Oxford 80 Plus) using gas flow of 15 standard cubic centimeters per minute (sccm) of CHF_3 and 5 sccm of Ar (the Ar component serves to stabilize the plasma). The plasma power and the chamber pressure were set at 200 W and 30 m Torr respectively for a total treatment period of 240 s. The remaining PR mask was then washed off and the plasma-treated devices (named light-structured LEDs in the rest of this paper) were wire bonded onto printed circuit boards for characterization.

Current versus voltage (I-V) characteristics under direct current (dc) drive conditions were measured with a Yokogawa GS610 source measure unit. In order to qualitatively investigate the surface modification effect, metal circular transmission line method (CTLM) semiconductor junctions were processed on the p-doped GaN surface from the same LED wafer using similar processing as for the LEDs. They consist of co-planar Ti (40 nm) /Au (150 nm) metal structures comprising circular pads, each with a concentric outer electrode of much larger area, separated by a $10 \mu\text{m}$ gap. Micro-photoluminescence (μPL) spectra were obtained using either a CW GaN-diode laser (PowerTechnologies) with a peak emission at 375 nm (10 mW nominal power) or a CW He-Cd laser (Plasma JSC) with a peak emission at 325 nm for the excitation source and an UV-visible spectrometer for the detection. The laser beam was focused on the sample with a 60X microscope objective (Nikon, CFI Plan FLuor) giving a spot diameter of $\sim 2 \mu\text{m}$ on the sample. The demonstration of maskless photolithography with LED direct exposure (also called *LED direct writing*) was made through an imaging setup with 10-to-1 demagnification capability using 4x and 40x microscope objectives for collection and projection, respectively, as described in previously reported work [5, 13]. The photolithography was performed on a silicon (Si) substrate coated successively with a SiO_2 layer and a layer of negative-tone PR (ma-N 1405 from Micro Resist Technology GmbH). The Si sample was placed at the focal plane underneath the projection optics and light emission from a 405 nm light-structured LED was used for the demonstration. The exposure dose was controlled by a shutter placed directly in front of the collection optics.

3. Results and discussion

3.1. Device performance and investigations of the p-GaN modification

Two examples of complex light emission patterns obtained using the process flow described above are presented in figures 1(b) and (c). Each complete image is emitted from one LED powered with a single cathode and anode, contrasting with the mode of image generation from pixelated micro-LED displays [2, 14]. Each fabricated LED shows a uniform brightness from the non-treated area, and no light emission from the plasma-treated area. The overall size of both

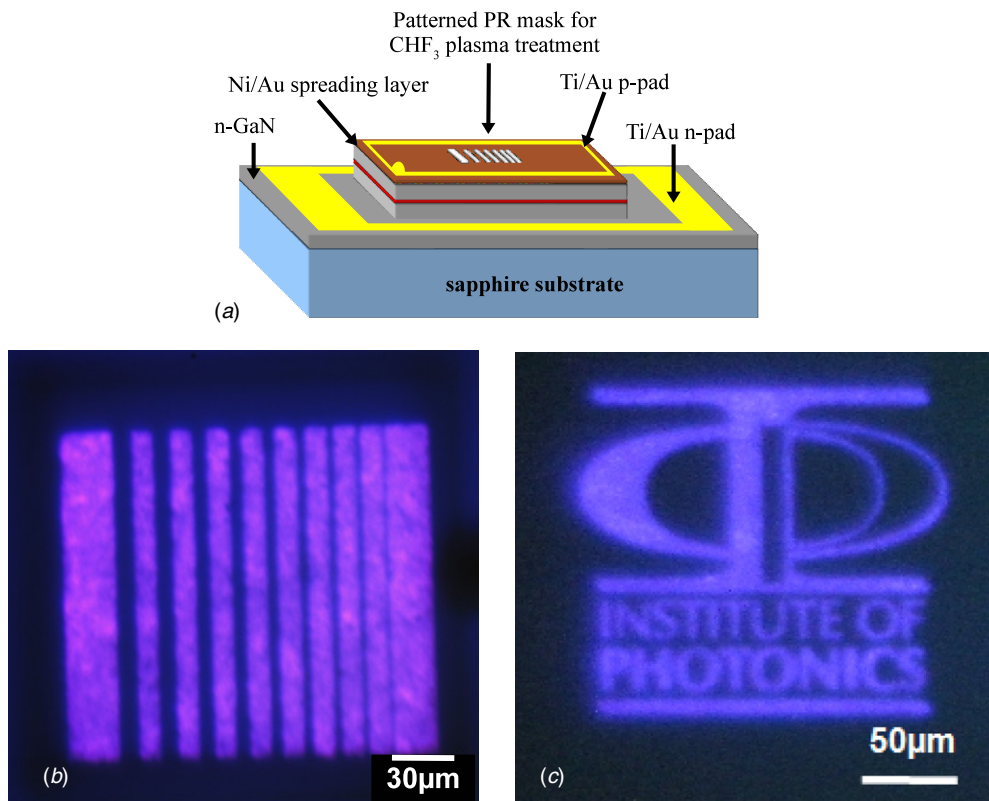


Figure 1. (a) Schematic structure of a LED with the patterned PR mask prior to the CHF_3 plasma treatment. (b) Optical micrographs showing a 1D array of bars and (c) the logo of our laboratory displayed respectively by 405 nm and 450 nm light-structured turned-on LEDs.

patterns is in the hundreds of micron range, and they show fine features as small as a few microns demonstrating a resolution already much better than the capabilities of pixelated micro-LED displays. Three other initial observations can be made about our process on the basis of the image display results. Firstly, a conventional polymer-based PR layer acts as an efficient mask for the room-temperature plasma treatment, and consequently this process is fully compatible with photolithography techniques used in standard microfabrication. Secondly, the unmasked NiO_x -Au layer coating the LED emitting surface does not show degradation induced by the plasma treatment and still performs its current-spreading purpose efficiently over the time of this study. Indeed, if the conductance of the current-spreading layer was somehow degraded, either through significant reduction of thickness or alteration of electrical properties, during the process, strong non-uniformity of light emission across the pixel would be expected as well as an important increase of the differential resistance. Further etching tests showed that over the timescale used for the plasma treatment, no measurable etching of the metallic current-spreading layer, nor of the p-GaN layer, could be detected. Finally, one can deduce that as a change in the electrical behavior of the spreading layer cannot explain the localization of light emission, an obvious inference is a strong modification of the electrical properties of the p-GaN layer induced by the plasma treatment. As the thin NiO_x -Au layer is expected to show high porosity after annealing [12], the plasma species can readily interact with the underlying p-GaN layer, leading to a spatial modulation of

the current injection efficiency, which in turn leads to a strong spatial modulation of the light emission.

Further optical and electrical studies were performed to investigate the effect of the CHF_3 -based plasma treatment. First, micro-PL measurements were done on treated and untreated areas of a light-structured LED. Excitation at 375 nm enables direct pumping of the quantum wells (QW) and therefore helps to assess if the plasma treatment causes any damage to the active region, while the 325 nm source excites mainly the p-type GaN layer. Indeed, 85% of the 325 nm pump light will be absorbed within a 200 nm thick p-type GaN layer and 25% within the first 30 nm. Results are shown in figure 2. It can be seen that the QW emission obtained under the 375 nm excitation (figure 2(a)) is basically identical in both treated and untreated regions. As both areas were only a few hundred microns apart for this measurement, the relative peak intensities are directly comparable and consequently it can be concluded that the plasma treatment has no effect on the optical properties of the QWs. Similarly, no clear difference can be noted under the 325 nm excitation as shown on figure 2(b) with the near band-edge emission (NBE) below 400 nm, the MQW emission centered at 450 nm and the common GaN's weak yellow luminescence centered at 580 nm [15]. In particular, the ratio between the NBE and the QWs emission remains constant, which is an indication that the carrier migration from the p-type GaN into the QW is unaffected by the plasma treatment. This means that either the hole mobility is not affected by the plasma treatment or that it has an effect only in a very thin layer (perhaps 30 nm or less) at the top of the p-type

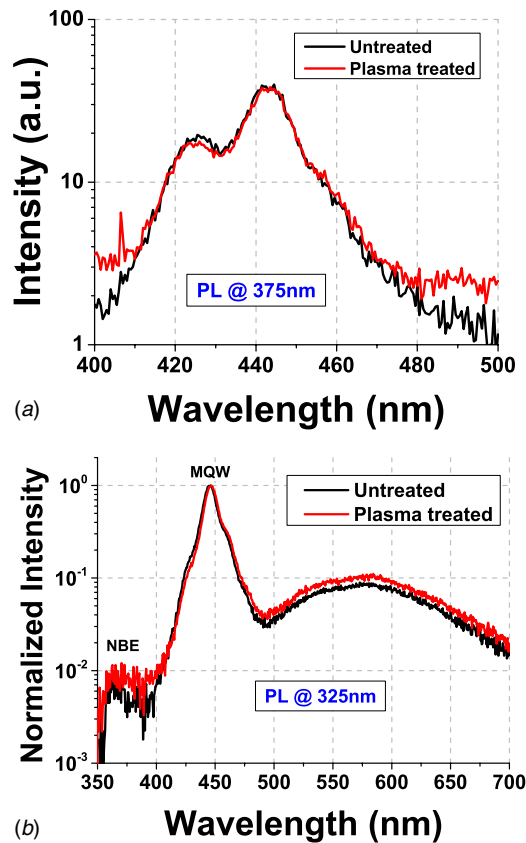


Figure 2. Micro-PL spectra of plasma-treated and untreated regions of a 450 nm LED excited respectively at 375 nm (a) and at 325 nm (b).

GaN layer. This interpretation is in agreement with studies by Chu *et al* [16] who observed a thin F-implanted surface layer.

For the electrical studies, CTLM structures, resulting in two Schottky metal–semiconductor junctions in series, were made as detailed in the experimental part above. These structures were made on the p-GaN surface of samples from the same wafer used to fabricate the 450 nm light-structured LEDs. Different pre-metallization plasma treatments were tested to elucidate the action of the CHF_3 plasma, and the resulting dc I–V characteristics are plotted in figure 3. Comparing the structure exposed to the CHF_3 plasma with the non-treated reference sample, a dramatic current reduction, by a factor exceeding 10^6 between 6 V and 10 V, was observed (comparisons are limited by the noise at lower currents), demonstrating that the CHF_3 plasma treatment enables a strong local inhibition of current injection over the whole operating range of standard GaN-based LEDs. Considered together with the PL results, we believe that the change in Schottky barrier behavior after the plasma treatment involves modification of the topmost layer of the p-GaN. Two complementary physical effects may contribute. The first is the well-known de-activation of Mg acceptors by hydrogen, which results in a decrease of the mobile hole concentration and thus of the p-GaN conductivity [8]. A second effect could be an increase of the effective metal–semiconductor barrier energy due to the implantation of fluorine into the p-GaN surface [16]. In order to evaluate these two possible effects in isolation, H_2 and CF_4

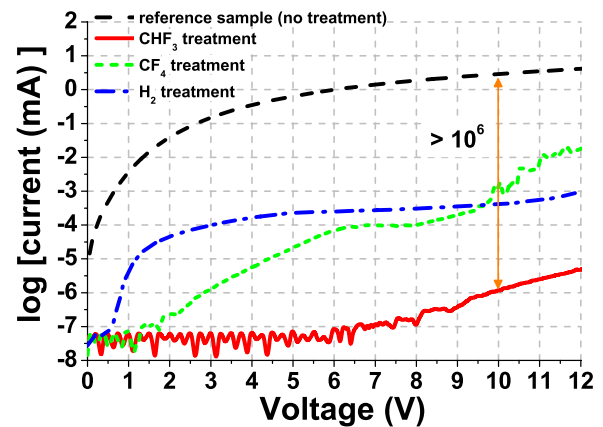


Figure 3. I–V characteristics of co-planar CTLM Ti/Au electrode structures deposited onto p-GaN and having undergone different pre-metallization plasma treatments.

plasma treatments were applied to two more structures, and the results are included in figure 3. In both cases, a significant reduction in current is observed compared to the untreated structure. However, the current blocking effect is significantly higher with the CHF_3 plasma treatment than with either the H_2 or the CF_4 treatments alone, which shows that it is likely that both effects happen simultaneously. Relating the behavior just discussed to the operation of our light-structured LEDs, the low lateral diffusion length of carriers in p-GaN [17] confines light emission to an area directly below or close to the point of current injection on the p-GaN surface. Consequently, one can easily understand that there is no light emission from the plasma treated area, in which vertical carrier injection is inhibited. As noted already, the semi-transparent NiO_x -Au current spreading layer over the p-GaN is not degraded by the plasma, and serves to electrically interconnect the untreated areas.

In order to illustrate the high resolution achievable by our technique, an array of disc emitters with decreasing nominal diameter down to $2 \mu\text{m}$ (the resolution limit of our mask aligner) was transferred using the CHF_3 plasma treatment onto a single LED. Figure 4(a) shows the line-scan of light intensity across the diameter of the smallest disc emitter as shown in the inset. This smallest emitter shows a full width at half maximum of $2.5 \mu\text{m}$, demonstrating the capability of the CHF_3 plasma treatment to fabricate elements comparable to the lithographic resolution limit. We anticipate that smaller emitters with sub-micron size could be fabricated with a higher resolution patterning technique such as e-beam, deep UV or nanoimprint lithography. Figure 4(b) shows the injection current versus forward bias voltage (I–V) characteristics for one LED before and after the image-transfer with the CHF_3 plasma treatment. The turn-on voltage of the LED ($\sim 3 \text{V}$) does not change during the process, demonstrating that the junction properties are unaffected by the plasma treatment, consistent with the results discussed already indicating a shallow modification depth for the p-GaN. However, an increase in the differential resistance r_d is clearly visible after the CHF_3 treatment to create localized emitting regions (dashed curve in figure 4(b)). As expected, the increase in r_d after plasma treatment depends on the area ratio

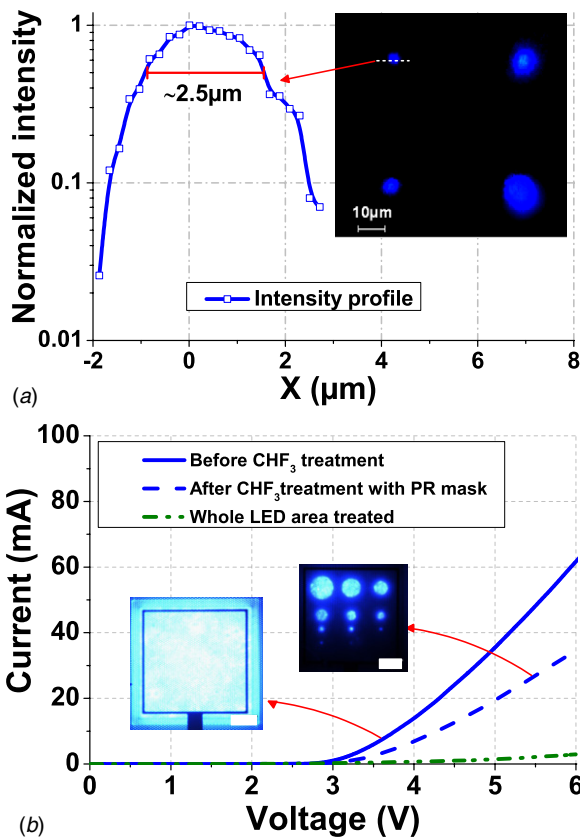


Figure 4. (a) Intensity profile across the diameter of the smallest emitting feature shown in the inset. The inset shows four microdisc-shape emitters with different diameters, fabricated by the CHF_3 plasma treatment on a single mesa. (b) I–V characteristics before and after CHF_3 plasma treatment of a single LED pixel. Emission pattern before and after CHF_3 treatment is shown in the inserted images. No light can be detected when the whole LED is plasma treated. Scale bars (white) in both images represent $50 \mu\text{m}$.

of exposed and mask-protected surface. The limiting case from a plasma treatment with no PR mask is shown in the figure; no visible light emission occurred although the current passed above turn-on is still detectable.

3.2. Maskless photolithography

Finally, the use of these light-structured LEDs was investigated for maskless photolithography, an application in which the compactness, high-brightness and high resolution of sources are key requirements. A 405 nm light-structured LED displaying $10 \mu\text{m}$ -wide bars separated by gaps of increasing width from $1 \mu\text{m}$ up to $10 \mu\text{m}$ (as shown in figure 1(b)) was used to investigate the resolution limit of the pattern transfer from the light-structured LED to a PR-coated sample using a custom-made imaging setup described previously [5]. An LED was driven at an injection current of 60 mA , providing an average optical power density of $\sim 1.3 \text{ W cm}^{-2}$ on the test sample placed at the focal plane. The exposure time was set to 3 s , giving an average exposure dose of $\sim 4 \text{ J cm}^{-2}$ similar to the dose deduced from the manufacturer's datasheet. After exposure, the sample was soaked 30 s in developer to reveal the pattern transferred and dried under air. Due to the negative-tone nature of the PR used, the area exposed to the LED light

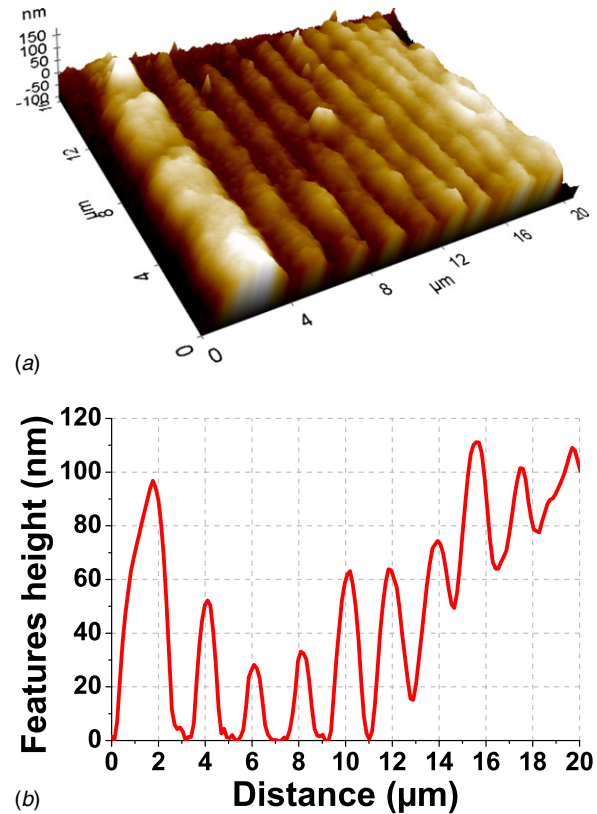


Figure 5. AFM image of the photoresist pattern made by maskless photolithography with a light-structured LED (a) and typical height profile extracted from the same image along the perpendicular direction to the stripes (b).

remains after development. The transferred pattern was then analyzed with an atomic force microscope (AFM) and a typical image is shown on figure 5(a). The extracted height profile is shown in figure 5(b). Due to the 10-to-1 demagnification, a perfect transfer would provide $1 \mu\text{m}$ -wide PR bars with intermediate gaps decreasing in width from $1 \mu\text{m}$ down to 100 nm . However because of the combined effects of non-ideality of the optical system, the divergence of the LED light emission and the diffraction limits, only the five largest gaps have been fully transferred into the PR layer, in the sense of the AFM probe reaching the Si substrate. The well-developed bars show a $\sim 1 \mu\text{m}$ -width at their base, as expected, with submicron gaps in-between down to $\sim 800 \text{ nm}$. The non-uniform thickness of the PR features is attributed in part to imperfect uniformity of the LED emission, but such pattern definition is already good enough for further processing steps, for example pattern transfer by dry-etching into a harder mask layer such as SiO_2 or metal. We anticipate that improved PR patterning could be obtained with further optimization of the imaging writing setup and process, as well as by using light-structured LEDs emitting at shorter wavelengths.

4. Conclusions

In summary, a new technique allowing the fabrication of single GaN-based LEDs with spatially microstructured light output patterns was demonstrated. This approach uses a

CHF₃-based plasma treatment at room temperature to modify the topmost p-GaN layer, leading to spatial modulation of current injection into the LED active region when some areas are protected from the plasma using a protecting patterned photoresist layer. Single devices fabricated in this manner can display images with micrometer resolution, while keeping electrical and optical performance similar to a unpatterned reference LEDs. Such a light-structured device emitting at 405 nm was used to demonstrate pattern transfer into PR by maskless photolithography. We anticipate that this new technique will be useful in a large range of applications with integrated optical sources, including micro-displays, bio-instrumentation, photolithography and lab-on-chip systems where compactness and low cost are of prime importance.

Acknowledgments

This work was supported by the UK EPSRC under the project EP/F05999X/1 'HYPIX'. Michael Wallace, Elaine Taylor and Paul Edwards from the University of Strathclyde department of Physics are acknowledged for their help in taking PL spectra at 325 nm excitation wavelength.

Q2 References

- [1] Crawford M H 2009 LEDs for solid-state lighting: performance challenges and recent advances *IEEE J. Select. Top. Quantum Electron.* **15** 1028–40
- [2] Choi H W, Jeon C W and Dawson M D 2004 High-resolution 128 × 96 nitride microdisplay *IEEE Electron. Device Lett.* **25** 277–9
- [3] McKendry J D, Massoubre D, Zhang S, Rae B R, Green R P, Gu E, Henderson R K, Kelly A E and Dawson M D 2012 Visible-light communications using a CMOS-controlled micro-light-emitting-diode array *IEEE J. Lighthwave Technol.* **30** 61–67
- [4] Zarowna-Dabrowska A *et al* 2011 Miniaturized optoelectronic tweezers controlled by GaN micro-pixel light emitting diode arrays *Opt. Express* **19** 2720–8
- [5] Guilhabert B, Massoubre D, Richardson E, McKendry J J D, Valentine G, Henderson R K, Watson I M, Erdan Gu and Dawson M D 2012 Sub-micron lithography using InGaN micro-LEDs: mask-free fabrication of LED arrays *IEEE Photon. Technol. Lett.* **24** 2221–4
- [6] Li Z L, Li K H and Choi H W 2010 Mechanism of optical degradation in microstructured InGaN light-emitting diodes *J. Appl. Phys.* **108** 114511
- [7] Pearton S J, Zolper J C, Shul R J and Ren F 1999 GaN: processing, defects, and devices *J. Appl. Phys.* **86** 1–78
- [8] Polyakov A Y, Smirnov N B, Govorkov A V, Pearton S J and Zavada J M 2003 Proton implantation effects on electrical and luminescent properties of p-GaN *J. Appl. Phys.* **94** 3069–74
- [9] Polyakov A Y, Smirnov N B, Govorkov A V, Baik K H, Pearton S J, Luo B, Ren F and Zavada J M 2003 Hydrogen plasma passivation effects on properties of p-GaN *J. Appl. Phys.* **94** 3060–965
- [10] Kuo T-W, Lin S-X, Hung P-K, Chong K-K, Hung C-I and Houg M-P 2010 Formation of selective high barrier region by inductively coupled plasma treatment on GaN-based light-emitting diodes *Japan. J. Appl. Phys.* **49** 116504
- [11] Cai Y, Zhou Y, Chen K J and Lau K M 2005 High-performance enhancement-mode AlGaIn/GaN HEMTs using fluoride-based plasma treatment *IEEE Electron. Device Lett.* **26** 435–7
- [12] Liday J, Hotový I, Sitter H, Schmidegg K, Vogrinčič P, Bonnani A, Breza J, Ecke G and Vávra I 2007 Auger electron spectroscopy of Au/NiO_x contacts on p-GaN annealed in N₂ and O₂ + N₂ ambients *Appl. Surf. Sci.* **253** 3174–80
- [13] Elfström D *et al* 2006 Mask-less ultraviolet photolithography based on CMOS-driven micro-pixel light emitting diodes *Opt. Express* **17** 23522–9
- [14] Day J, Li J, Lie D Y C, Bradford C, Lin J Y and Jiang H X 2011 III-nitride full-scale high-resolution microdisplays *Appl. Phys. Lett.* **99** 031116
- [15] Grieshaber W, Schubert E F, Goepfert I D, Karlicek R F, Schurman M J and Tran C 1996 Competition between band gap and yellow luminescence in GaN and its relevance for optoelectronic devices *J. Appl. Phys.* **80** 4615–20
- [16] Chu R, Suh C S, Wong M H, Fichtenbaum N, Brown D, McCarthy L, Keller S, Wu F, Speck J S and Mishra U K 2007 Impact of CF₄ plasma treatment on GaN *IEEE Electron. Device Lett.* **28** 781–3
- [17] Hickmana R *et al* 2000 GaN PN junction issues and developments *Solid-State Electron.* **44** 377–81

QUERIES

Page 1

Q1

Author: Please be aware that the color figures in this article will only appear in color in the Web version. If you require color in the printed journal and have not previously arranged it, please contact the Production Editor now.

Page 6

Q2

Author: Please check the details for any journal references that do not have a blue link as they may contain some incorrect information. Pale purple links are used for references to arXiv e-prints.